Solvent-Induced On/Off Switching of Intramolecular Electron Transfers in a Cyanide-Bridged Trigonal Bipyramidal Complex

Rong-Jia Wei,[a] Ryohei Nakahara,[a] Jamie M. Cameron,[a] Graham N. Newton,[a,b] Takuya Shiga,[a] Hajime Sagayama,[c] Reiji Kumai,[c] Youichi Murakami,[c] and Hiroki Oshio*[a]

a. Graduate School of Pure and Applied Sciences, University of Tsukuba, Tsukuba 305-8571, Japan.

b. School of Chemistry, The University of Nottingham, University Park, UK

c. Photon Factory and Condensed Matter Research Center, Institute of Materials Structure Science, High Energy Accelerator Research Organization (KEK), Tsukuba 305-0801, Japan

E-mail: oshio@chem.tsukuba.ac.jp

Table of Contents

Materials and Physical Measurements.

All reagents were obtained from commercial suppliers and were used without further purification. Variable-temperature magnetic susceptibility measurements were carried out on polycrystalline samples under an applied field of 1 T using a Quantum Design MPMS-XL SQUID magnetometer. Pascal's constants were used to determine the diamagnetic corrections. Data collections were conducted at a rate of 1 K/min. Mössbauer experiments were carried out using a ^{57}Co/Rh source in a constant acceleration transmission spectrometer (Topologic Systems) equipped with an Iwatani HE05/CW404 Cryostat. The spectrometer was calibrated using standard α-Fe foil at room temperature. Thermogravimetric analysis (TGA) was conducted under an Ar flow using an EXSTAR TG/DTA7300 thermogravimetric analyser heating from room temperature with a scan rate of 5 K /min. Elemental analyses for C, H, and N were performed on Perkin-Elmer 240Q elemental analyzer. The IR spectra (KBr pellets, 4000 – 400 cm^{-1}) were recorded by using a Shimadzu Model IR Affinity-1 spectrometer. Synchrotron X-ray diffractometer measurements were performed using a diffractometer at room temperature installed at BL-8A at the Photon Factory, KEK, Tsukuba. The wavelength of the incident synchrotron X-ray beam, monochromated by a Si (111) double-crystal monochromator, was set to 1.0000 Å and the X-ray diffractions were detected using an IP area detector.

Syntheses.

A solution of 2-pyridinecarbaldehyde (71.1 μL, 0.75 mmol) and (*S*)-(+)-1,2,3,4-Tetrahydro-1-naphthylamine (95.7 μL, 0.75 mmol) in 3.0 mL ethanol was combined with a solution of $CoCl_2 \cdot 6H_2O$ (85.2 mg, 0.25 mmol) in 3.0 mL ethanol to give a red solution which was allowed to stir for 5 min and then combined with a solution of $(Et_4N)_3[Fe(CN)_6]$ (301 mg, 0.50 mmol) and $(Et_4N)ClO_4$ (301 mg, 0.50 mmol) in 4.0 mL ethanol. The resulting green solution was left to stand and red needle crystals suitable for X-ray single-crystal diffraction were obtained in three days and collected by filtration. Yield: 11 mg (10 %). Elemental analysis (%) calcd for $C_{116}H_{116}ClCo_3Fe_2N_{25}O_4 \cdot 9C_2H_5OH \cdot 4H_2O$ (4 EtOH solvent molecules are exchanged with water from air): C 58.85, H 6.56, N 12.80; found: C 58.84, H 6.54, N 12.84. IR (KBr,): 2148, 2118, 2063, 1639, 1095.

After drying **1** under N_2 for three hours, red crystals of $\mathbf{1}^{de}$ were obtained. Elemental analysis (%) calcd for $C_{116}H_{116}ClCo_3Fe_2N_{25}O_4 \cdot 7H_2O$ (the EtOH solvent molecules are exchanged with water from air): C 58.68, H 5.52, N 14.75; found: C 58.64, H 5.62, N 14.55.

The re-adsorbed sample $\mathbf{1}^{re}$ was obtained by exposing dry sample of $\mathbf{1}^{de}$ to EtOH vapor for one day. Elemental analysis (%) calcd for $C_{116}H_{116}ClCo_3Fe_2N_{25}O_4 \cdot 7C_2H_5OH \cdot 7H_2O$: C 57.96, H 6.43, N 12.98; found: C 58.05, H 6.50, N 13.22.

Single Crystal X-ray Structural Analyses.

A red single crystal of **1** was picked up from mother liquor, and sealed into glass capillary with small amount of mother solvent, and diffraction data for LT phase (the crystal turned to green due to ETCST) were collected at 100 K using a Bruker SMART APEXII diffractometer coupled with a CCD area detector with graphite monochromated Mo *K*α (λ = 0.71073 Å) radiation. Subsequently, the temperature of the cooling stream was increased slowly at a rate of 1 K / min to 300 K, and diffraction data for the HT phase (in red colour)

were collected.

A single crystal of as-synthesized **1** was selected from mother liquor and mounted without coating agents under a nitrogen cooling spray at 100 K. Unit-cell parameters of the sample were measured to confirm it was in solvated form as expected. Subsequently, the temperature of the cooling stream was increased slowly to 270 K and the cell constants were monitored. Changes in cell parameters were observed for the crystal after three hours drying, and diffraction data of **1**^{de} were collected after the cooling stream was decreased to 100 K (the crystal kept in red).

The structures were solved using direct methods and expanded using Fourier techniques within the SHELXTL program.[1] Empirical absorption corrections were calculated using SADABS. In the structure analyses, non-hydrogen atoms were refined with anisotropic thermal parameters. Hydrogen atoms were included in calculated positions and refined with isotropic thermal parameters riding on those of the parent atoms. DELU, SIMU and DFIX commands are applied during refinement to fix the ADP and disorder problems arising from the weak diffraction data for the structure of **1** in HT phase and **1**^{de}. Electron density contributions from the highly disordered solvent molecules for **1** in HT phase and **1**^{de} were handled using the "SQUEEZE" procedure[2] from the PLATON software. Large R1 and wR2 values (0.1655 and 0.4256, respectively) were observed for **1**^{de} are due to possible crystalline decay and weak diffraction arisen from solvent release. However, the atoms and geometric features for the [Co_3Fe_2] cluster in **1**^{de} can be finely defined and no A-level alerts were observed except the CHEMW03 alert arising from the use of SQUEEZE.

*Details of "Squeeze" for **1** at 300 K.*

Approximately 38.4 % of the unit cell volume comprises a large region of disordered solvent that could not be modeled as discrete atomic sites. We employed PLATON SQUEEZE[2] to calculate the contribution to the diffraction from the solvent region and thereby produced a set of solvent-free diffraction intensities. SQUEEZE estimated a total count of 1309.7 electrons per unit cell which were assigned to 13 EtOH molecules per cluster.

*Details of "Squeeze" for **1**^{de} at 100 K.*

Approximately 12.5 % of the unit cell volume comprises a large region of disordered solvent that could not be modeled as discrete atomic sites. We employed PLATON SQUEEZE[2] to calculate the contribution to the diffraction from the solvent region and thereby produced a set of solvent-free diffraction intensities. SQUEEZE estimated a total count of 497.4 electrons per unit cell which were assigned to 5 EtOH molecules per cluster.

Table S1. Selected Interatomic Distances [Å] in **1** and **1**^{de}.

	1 at 100 K	**1** at 300 K	**1**^{de} at 100 K
Co1-N1	1.942(8)	2.152(6)	2.128(9)
Co1-N2	1.947(8)	2.149(9)	2.20(2)
Co1-N3	1.962(9)	2.191(9)	2.22(2)
Co1-N4	1.936(8)	2.160(6)	2.170(8)
Co1-N5	1.885(8)	2.08(1)	2.12(2)
Co1-N6	1.873(9)	2.084(9)	2.07(1)

Co1-N (average)	1.924	2.135	2.150
Co2-N7	1.943(8)	2.10(1)	2.17(2)
Co2-N8	1.943(8)	2.181(7)	2.12 (1)
Co2-N9	1.963(9)	2.129(6)	2.126(7)
Co2-N10	1.951(8)	2.16(1)	2.10(2)
Co2-N11	1.881(8)	2.00(1)	2.05(1)
Co2-N12	1.889(8)	2.044(9)	1.99(1)
Co2-N (average)	1.928	2.101	2.095
Co3-N13	2.138(9)	2.162(6)	2.14(1)
Co3-N14	2.201(8)	2.178(8)	2.27(2)
Co3-N15	2.167(7)	2.128(9)	2.28(2)
Co3-N16	2.176(8)	2.103(9)	2.165(9)
Co3-N17	2.042(8)	2.057(9)	2.05(2)
Co3-N18	2.027(8)	2.059(9)	1.95(2)
Co2-N (average)	2.125	2.114	2.141
Fe1-C97	1.89(1)	1.92(1)	1.96(2)
Fe1-C98	1.88(1)	1.90(1)	1.93(1)
Fe1-C99	1.89(1)	1.95(1)	1.92(2)
Fe1-C100	1.92(1)	1.97(1)	1.90(2)
Fe1-C101	1.91(1)	1.98 (1)	1.96(2)
Fe1-C102	1.94(1)	1.9671)	1.91(2)
Fe1-N (average)	1.906	1.946	1.929
Fe2-C103	1.873(9)	1.99(1)	1.91(1)
Fe2-C104	1.88(1)	1.93(1)	1.98(2)
Fe2-C105	1.89(1)	1.97(1)	1.89(2)
Fe2-C106	1.92(1)	1.92(1)	1.86(2)
Fe2-C107	1.92(1)	1.94(1)	1.92(2)
Fe2-C108	1.94(1)	1.87(1)	1.98(2)
Fe2-N (average)	1.904	1.936	1.923

Table S2. Selected angles of the Co and Fe sites in **1** and **1**^{de}. The variations of the geometries have been quantified using the octahedral distortion parameter, Σ, a parameter determining the angular deviation from octahedral geometry (calculated by the sum of the deviation of each of the 12 *cis* angles from 90º). For the solvated sample 1, the Σ values at 300 K are significant larger than those at 100 K for Co1 and Co2, but almost constant for Co3, indicating electron transfers occurred on the Co1 and Co2 sites. In contract, the Σ values at 300 K are smaller than those at 100 K for the Fe sites. For **1**^{de}, the Σ values are all larger than those in **1**.

	1 at 100 K	**1** at 300 K	**1**^{de} at 100 K
N6-Co1-N5	89.4(2)	89.8(2)	90.1(5)
N6-Co1-N4	92.9(3)	91.8(3)	92.8(4)

N5-Co1-N4	92.8(2)	99.48(19)	101.4(5)
N6-Co1-N1	90.2(2)	97.8(2)	100.1(5)
N5-Co1-N1	92.9(2)	92.2(3)	91.4(5)
N6-Co1-N2	88.1(2)	86.0(3)	83.6(5)
N4-Co1-N2	91.9(3)	93.4(3)	89.9(5)
N1-Co1-N2	82.5(3)	75.7(3)	79.0(6)
N5-Co1-N3	88.7(2)	90.7(2)	87.1(5)
N4-Co1-N3	82.1(3)	77.0(2)	74.8(5)
N1-Co1-N3	95.0(3)	93.4(2)	93.2(5)
N2-Co1-N3	94.2(3)	95.9(2)	101.5(5)
Σ_{Co1}	39.1	66.2	76.1
N11-Co2-N12	89.9(2)	93.9(2)	91.8(5)
N11-Co2-N7	94.0(2)	96.4(3)	97.4(6)
N12-Co2-N7	85.3(2)	87.0(3)	90.2(6)
N12-Co2-N8	91.2(2)	90.0(2)	91.8(5)
N7-Co2-N8	82.3(3)	75.8(3)	92.0(5)
N11-Co2-N10	85.9(2)	88.4(3)	76.2(5)
N12-Co2-N10	95.1(2)	94.0(3)	85.8(4)
N8-Co2-N10	97.7(2)	79.5(3)	85.8(5)
N11-Co2-N9	91.4(2)	90.6(2)	90.3(5)
N7-Co2-N9	97.0(3)	99.1(3)	77.9(5)
N8-Co2-N9	87.7(2)	86.5(2)	100.6(4)
N10-Co2-N9	82.7(3)	99.3(3)	101.4(6)
Σ_{Co2}	52.6	66.1	69.8
N18-Co3-N17	91.6(2)	90.9(2)	90.9(6)
N18-Co3-N13	101.3(2)	97.4(2)	97.6(5)
N17-Co3-N13	92.2(2)	91.2(3)	89.4(5)
N17-Co3-N15	94.4(2)	89.1(2)	91.3(5)
N13-Co3-N15	92.0(2)	91.4(3)	97.1(6)
N18-Co3-N16	90.6(2)	98.1(2)	96.2(6)
N17-Co3-N16	100.1(2)	98.8(2)	96.4(6)
N15-Co3-N16	75.1(2)	76.5(3)	77.5(5)
N18-Co3-N14	84.8(2)	94.9(3)	84.2(6)
N13-Co3-N14	76.9(2)	84.1(2)	87.4(6)
N15-Co3-N14	92.1(2)	96.0(3)	100.6(7)
N16-Co3-N14	91.8(2)	75.7(3)	75.6(5)
Σ_{Co3}	69.3	73.3	76
C98-Fe1-C97	88.9(3)	88.1(3)	89.0(9)
C98-Fe1-C99	88.7(3)	93.6(3)	89.0(8)
C97-Fe1-C99	92.6(3)	90.3(3)	91.4(7)
C97-Fe1-C101	88.9(3)	90.2(4)	89.8(9)

C99-Fe1-C101	89.3(3)	93.0(4)	92.2(7)
C98-Fe1-C100	89.5(3)	87.8(3)	87.9(9)
C99-Fe1-C100	94.7(3)	87.2(3)	94.2(8)
C101-Fe1-C100	92.8(3)	89.6(3)	85.2(7)
C98-Fe1-C102	90.0(3)	90.6(3)	90.2(8)
C97-Fe1-C102	84.1(3)	88.4(3)	89.0(10)
C101-Fe1-C102	91.9(3)	91.0(3)	89.1(8)
C100-Fe1-C102	88.6(3)	90.2(3)	93.1(8)
Σ_{Fe1}	24	17.8	22.1
C103-Fe2-C104	92.6(3)	87.7(3)	89.6(8)
C103-Fe2-C105	87.9(3)	89.6(3)	89.2(7)
C104-Fe2-C105	87.7(3)	88.4(3)	94.3(6)
C103-Fe2-C107	87.0(3)	89.8(3)	93.2(8)
C105-Fe2-C107	89.4(3)	90.7(3)	85.1(7)
C103-Fe2-C106	91.3(3)	89.2(3)	85.4(7)
C104-Fe2-C106	88.2(3)	90.4(3)	83.3(6)
C107-Fe2-C106	94.7(3)	90.1(3)	91.9(7)
C104-Fe2-C108	89.7(3)	89.1(3)	92.8(8)
C105-Fe2-C108	89.5(3)	88.3(3)	86.7(8)
C107-Fe2-C108	90.5(3)	92.6(3)	93.7(9)
C106-Fe2-C108	91.4(3)	94.0(3)	94.8(7)
Σ_{Fe2}	21.1	15.7	44.4

Table S3. Mössbauer parameters of **1**, **1**^{de} and **1**^{re}. Least-squares-fit parameters: δ_{IS}, ΔE_Q, Γ and A are isomer shifts, quadrupole splitting, Lorentzian line width and area ratio, respectively. Parameters were calculated relative to α–Fe foil.

		δ_{IS} (mm s^{-1})		ΔE_Q (mm s^{-1})		Γ (mm s^{-1})		A (%)	
		Fe^{II}_{LS}	Fe^{III}_{LS}	Fe^{II}_{LS}	Fe^{III}_{LS}	Fe^{II}_{LS}	Fe^{III}_{LS}	Fe^{II}_{LS}	Fe^{III}_{LS}
1	(100 K)	0.00	-	0.20	–	0.27	–	100	–
	(260 K)	-0.05	-0.07	0.14	0.56	0.28	0.36	55	45
	(300 K)	–	-0.14	–	0.56	–	0.38	–	100
1de	(100 K)	–	-0.07	–	0.88	–	0.49	–	100
1re	(100 K)	-0.01	–	0.18	–	0.35	–	100	–

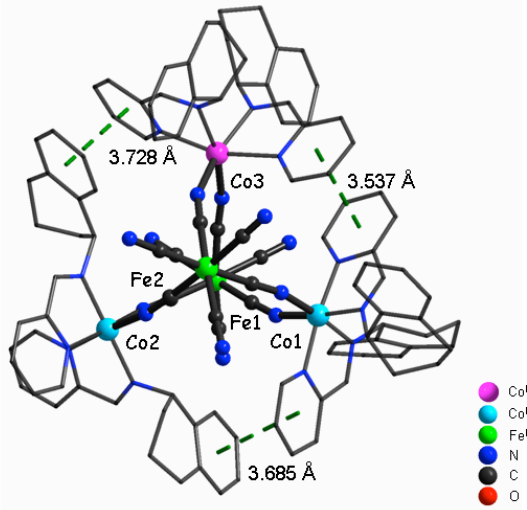

Fig. S1 Intramolecular π−π stacking interactions at 100 K (shown in centroid-to-centroid distances) between the neighbouring pyridine groups of the ligands, which help to stabilize the molecule's trigonal bipyramidal geometries.

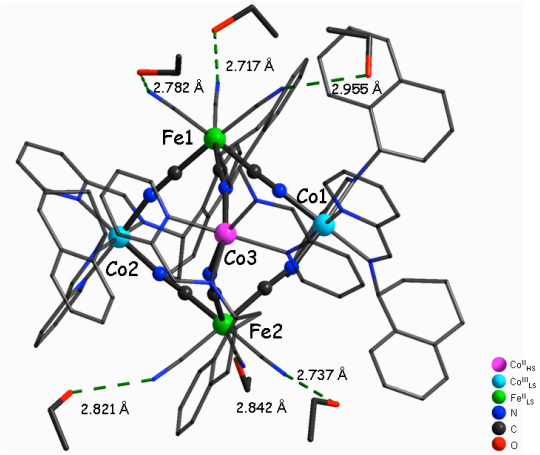

Fig. S2 Hydrogen bonding interactions (interatomic distances) between the $[Co_3Fe_2]$ cluster and the lattice EtOH molecules at 100 K.

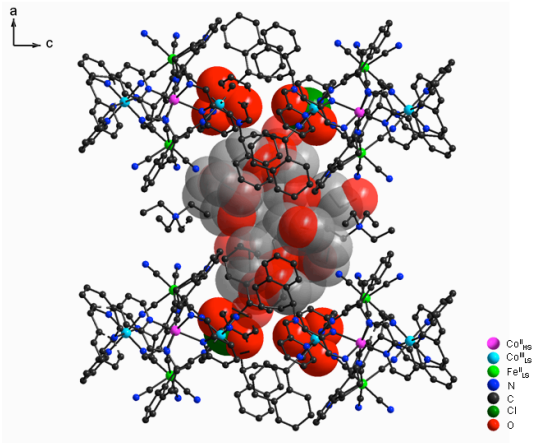

Fig. S3 Crystal packing diagram of **1** at 100 K. The $[Co_3Fe_2]$ clusters and $[Et_4N]^+$ cations stack alternately to form one-dimensional chains along the *a* axis, and the void space is occupied by ClO_4^- counter-anions and uncoordinated EtOH solvent molecules.

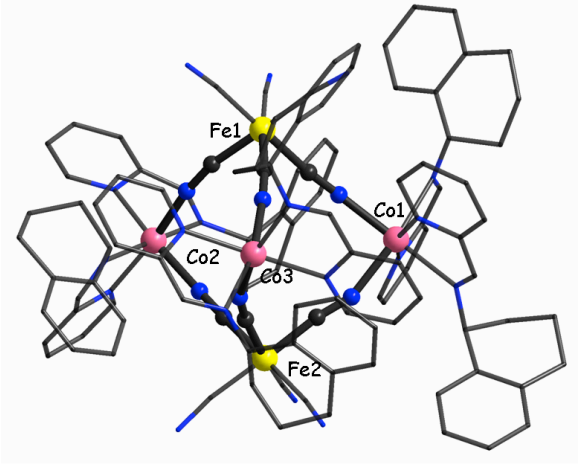

Fig. S4 Molecular structure of **1**^{de} at 100 K. The hydrogen atoms, $(Et_4N)^+$, ClO_4^-, and solvent molecules have been omitted for clarity.

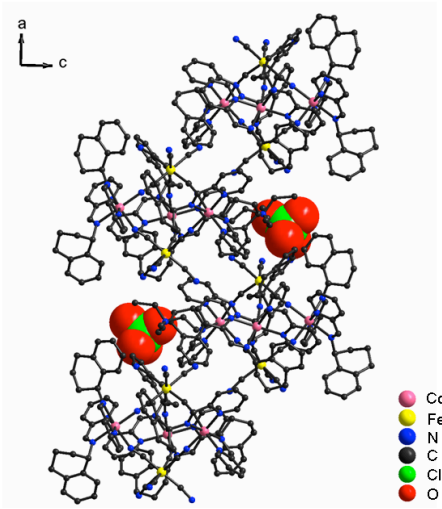

Fig. S5 Crystal packing diagram of **1**^{de}. Similar to **1**, the complex shows a one-dimensional chain structure consisting of alternately stacking $[Co_3Fe_2]$ clusters and $[Et_4N]^+$ cations along the *a*-axis. However, the chains in **1**^{de} show a compact stacking feature along the *c*-axis, resulting in a smaller void space for solvent molecule to occupy.

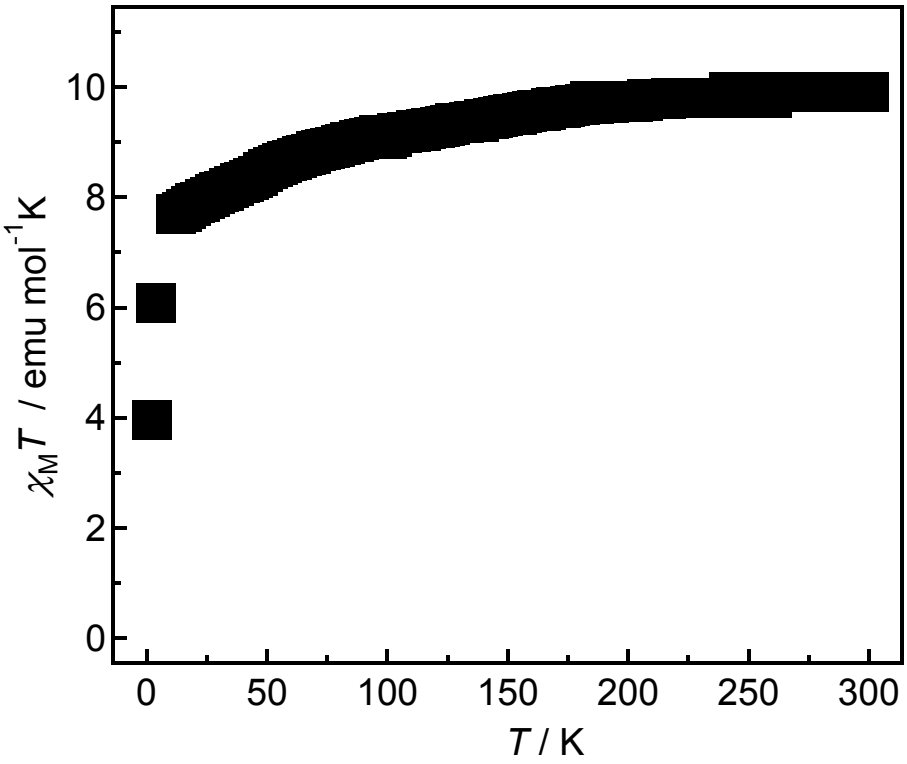

Fig. S6 $\chi_M T$ versus T plots for the fully dry [Co_3Fe_2] complex.

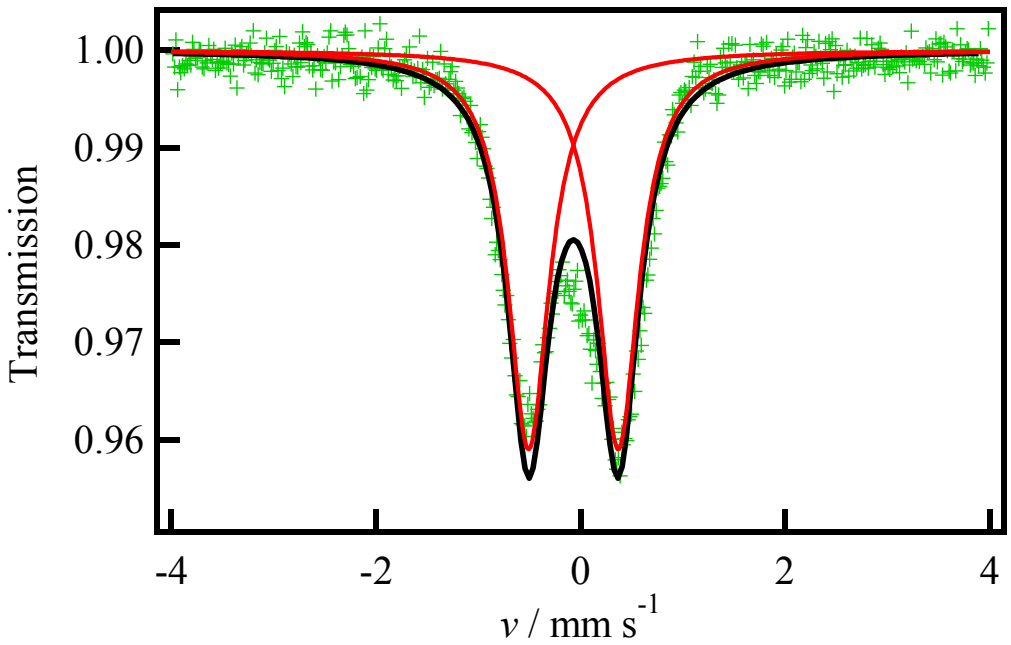

Fig. S7 Mössbauer spectrum at 100 K for **1**^{de}. Mössbauer parameters (δ_{IS} = -0.07 mms^{-1} and ΔE_Q = 0.88 mm s^{-1}) suggest the Fe ions are in the Fe^{III}_{LS} state.

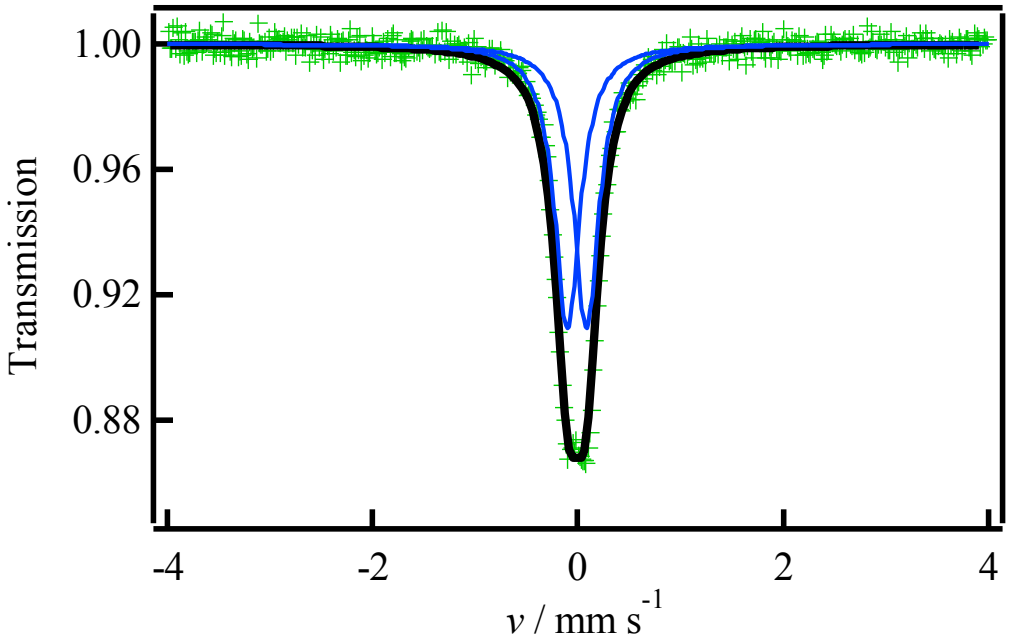

Fig. S8 Mössbauer spectrum at 100 K for $\mathbf{1}^{re}$. Mössbauer parameters (δ_{IS} = -0.01 mms^{-1} and ΔE_Q = 0.18 mm s^{-1}) suggest the Fe ions are in the Fe^{II}_{LS} state.

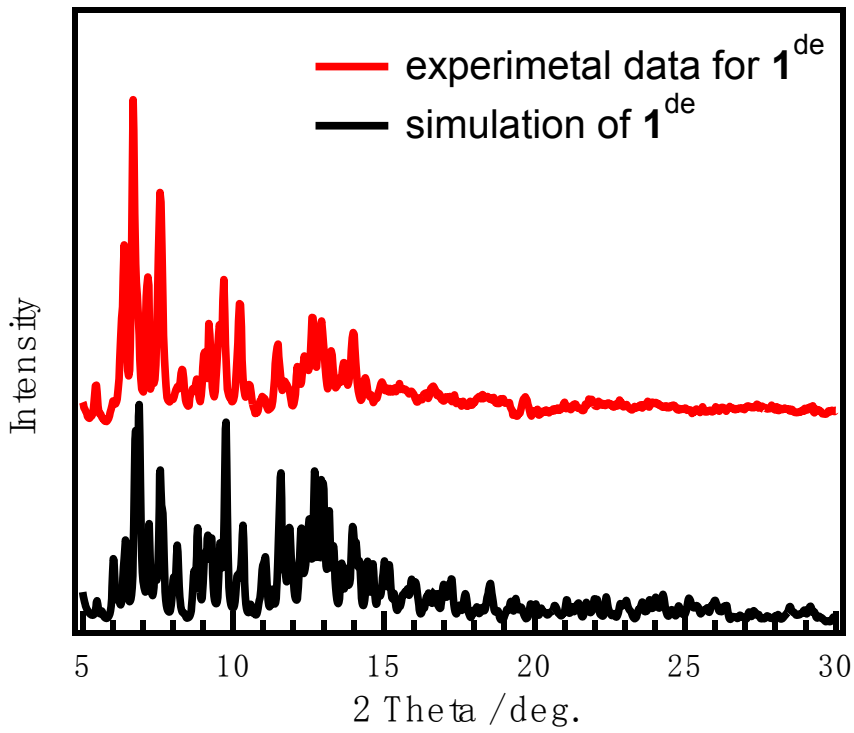

Fig. S9 Synchrotron powder XRD pattern of the desolvated sample $\mathbf{1}^{de}$ (red line) compared to the simulated result (black line, λ = 1 Å) from single-crystal data of $\mathbf{1}^{de}$.

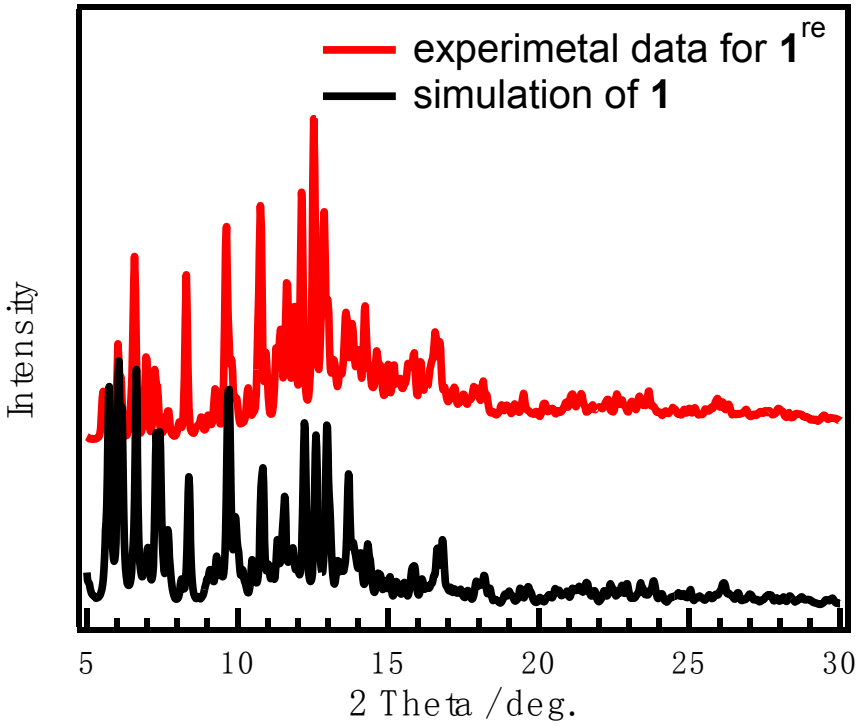

Fig. S10 Synchrotron powder XRD pattern of the EtOH-re-absorbed $\mathbf{1}^{re}$ (red line), compared to the simulated result (black line, λ = 1 Å) from single-crystal data of as-synthesized **1**.

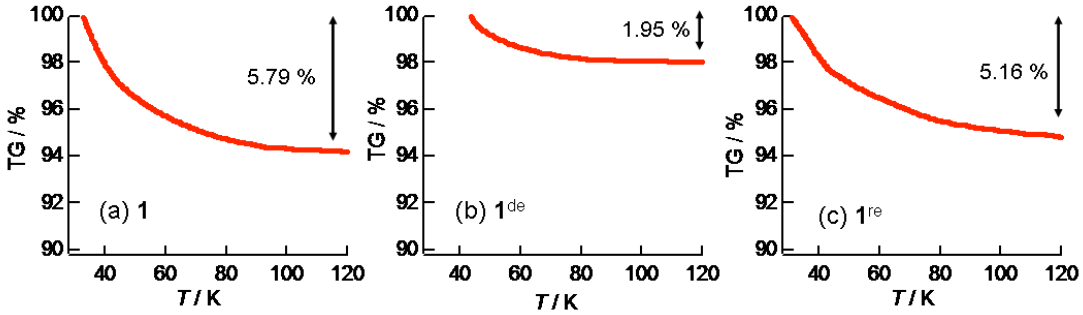

Fig. S11 Thermal gravimetric (TG) analyses of (a) **1**, (b) $\mathbf{1}^{de}$ and (c) $\mathbf{1}^{re}$ in Ar atmosphere, respectively. The complexes begin to lose weight at room temperature, revealing the lattice solvent molecules of the complexes are easily released upon the flow of Ar. As a result, the weight losses for the complexes are not consistent with the expected values: 21.0 % (13 EtOH), 9.3 % (5 EtOH) and 16.6 % (7 EtOH and 7H_2O) for **1**, $\mathbf{1}^{de}$ and $\mathbf{1}^{re}$, respectively.

Reference.

1. G. M. Sheldrick, *Acta Crystallogr.,* 2008, **A64**, 112.
2. A. L. Spek, *Acta Crystallogr.,* 2009, **D65**, 148.